Research Square

Preprints are preliminary reports that have not undergone peer review.
They should not be considered conclusive, used to inform clinical practice,
or referenced by the media as validated information.

The Role of Sirtuin 1 in Palmitic-acid-induced Endoplasmic-reticulum Stress in Cardiac Myoblasts

Hsiang-Yu Yang
National Defense Medical Center
Jhao-Ying Chen
National Defense Medical Center
Yen-Nien Huo
Taipei Medical University
Pei-Ling Yu
National Defense Medical Center
Pei-Zhen Lin
National Defense Medical Center
Shih-Che Hsu
CVie Therapeutics Ltd
Shih-Ming Huang
National Defense Medical Center
Chien-Sung Tsai
National Defense Medical Center
Chih-Yuan Lin (linrock@ms26.hinet.net)
National Defense Medical Center

Research Article

Keywords: Palmitate, endoplasmic reticulum stress, sirtuin 1

Posted Date: August 12th, 2021

DOI: https://doi.org/10.21203/rs.3.rs-785632/v1

License: This work is licensed under a Creative Commons Attribution 4.0 International License.
Read Full License

Version of Record: A version of this preprint was published at Life on January 26th, 2022. See the published version at https://doi.org/10.3390/life12020182.

Abstract

Background: Lipotoxicity causes endoplasmic reticulum (ER) stress, leading to cell apoptosis. Sirtuin 1 (Sirt1) regulates gene transcription and cellular metabolism. In this study, we investigated the role of Sirt1 in palmitate-induced ER stress.

Methods: H9c2 myoblasts and heart-specific *Sirt1* knockout mice fed a palmitate-enriched high-fat diet were used.

Results: The high-fat diet induced C/EBP homologous protein (CHOP) and activating transcription factor 4 (ATF4) expression in both Sirt1 knockout mice and controls. Sirt1 knockout mice showed higher CHOP and ATF4 expression compared to those in control. Palmitic acid (PA) induced ATF4 and CHOP expression in H9c2 cells. PA-treated H9c2 cells showed decreased cytosolic NAD^+/NADH alongside reduced Sirt1's activity. H9c2 cells showed increased ATF4 and CHOP expression when transfected with plasmid encoding dominant negative mutant Sirt1. Sirt1 activator SRT1720 did not affect CHOP and ATF4 expression. Although SRT1720 enhanced nuclear translocation of ATF4, the extent of the binding of ATF4 to the *CHOP* promoter did not increase further in PA treated-H9c2 cells.

Conclusion: PA-induced ER stress is mediated through upregulation of ATF4 and CHOP. Cytosolic NAD^+ concentration is diminished by PA-induced ER stress, leading to decreased Sirt1 activity. The Sirt1 activator SRT1720 promotes nuclear translocation of ATF4 in PA-treated H9c2 cells.

1 Introduction

Cardiac lipotoxicity, featuring toxic lipid accumulation in the heart, plays a pathological role in the development of obesity-induced cardiovascular diseases[1]. Saturated fatty acids, especially 16-C palmitate, are reported to be more lipotoxic than unsaturated fatty acids in cardiomyocytes[2]. A major mechanism underlying the palmitate-induced cardiomyocyte dysfunction is endoplasmic reticulum (ER) stress, which may promote cell death[3].

ER stress results from excessive accumulation of misfolded proteins within the ER and triggers a compensatory mechanism, the unfolded protein response (UPR), intended to modulate ER stress and restore ER homeostasis[4]. ER transmembrane proteins, including PKR-like ER kinase (PERK), activating transcription factor 6 (ATF6), and inositol-requiring enzyme 1 (IRE1), are responsible for UPR initiation. The UPR may switch to a proapoptotic signaling pathway to terminate the cell dysfunction. In the apoptosis pathways, activating transcription factor 4 (ATF4) plays a crucial role because it drives the transcription of a number of apoptosis genes, including a proapoptotic one, C/EBP homologous protein (*CHOP*), also known as DNA damage–inducible transcript 3 protein.

Sirtuin 1 (Sirt1) is a member of the sirtuin family and is an NAD^+-dependent enzyme performing the deacetylation of target substrates by hydrolyzing NAD^+ to produce a deacetylated substrate, acetyl-ADP-

ribose, and nicotinamide. Sirt1 is capable of deacetylating acetyl-lysine in histones, such as H3K9Ac, for gene transcription modulation. Sirt1 plays an important part in the regulation of cellular metabolism, inflammation, the cell cycle, and DNA repair[5]. Impairment of cardiac Sirt1 signaling is reported to contribute to the pathogenesis of cardiovascular diseases[6–8]. Sirt1 has also been shown to provide cardioprotection against ER stress–induced cell death through eIF2α deacetylation in a Sirt1 knockout mouse model[9].

The aim of the present study was to investigate the mechanism of palmitate-induced ER stress in cardiomyocytes and to determine the role of Sirt1. Here, we used H9c2 myoblasts and mice with a heart-specific *Sirt1* exon-4 knockout fed a palmitate-enriched high-fat diet (HFD) to identify the signaling pathway involved in palmitic acid (PA)-induced ER stress. We tested whether Sirt1 expression is affected by PA-induced ER stress and explored possible protective effects of Sirt1. We hope that our current findings provide a novel insight into PA-induced ER stress and into the function of Sirt1 in cardiomyocytes.

2 Methods

2.1 Genetically modified and HFD mouse models

Animal experiments were all conducted with the approval of the Institutional Animal Care and Use Committee (IACUC, permit No. 19–364) of the National Defense Medical Center (Taipei, Taiwan) and in accordance with the National Institutes of Health guidelines, “Guide for the Care and Use of Laboratory Animals,” on manipulations with experimental animals. The study was carried out in compliance with the ARRIVE guidelines

The mice with the heart-specific *Sirt1* exon-4 knockout ($Sirt1^{-/-}$) were created by crossing $Sirt1^{flox/flox}$ mice (controls purchased from Jackson Laboratory) with mice carrying α-MHC (myosin heavy chain) promoter–driven *Cre* in a C57BL/6J background (α-MHC-Cre mice, courtesy of Prof. M. Schneider, Imperial College London) and are currently in use in the laboratory[10]. Six-week-old mice were separately fed either a standard diet (SD) (10% kcal fat, D17071303i, Research Diets, USA) or a palmitate-enriched HFD (60% kcal fat, D16042106i, Research Diets, USA) for 8 weeks and then were euthanized to collect the hearts for subsequent experiments. The animals were kept at a temperature of 21 ± 1°C on a controlled 12:12 h light-dark cycle with *ad libitum* access to deionized drinking water before the experiments.

2.2 Cardiomyocyte isolation

Ventricular myocytes were enzymatically dissociated as previously described[11], with modifications. Briefly, mice were euthanized using a mixture of Zoletil 50 and xylazine, and the hearts were excised and cannulated via the aorta to a Langendorff perfusion system at 37°C. Each heart was first perfused with normal Tyrode’s solution (137 mM NaCl, 1.8 mM $CaCl_2$, 0.5 mM $MgCl_2$, 5.4 mM KCl, 10 mM glucose, and 10 mM HEPES [pH adjusted to 7.4 with NaOH]) for 10 min and digested with a Ca^{2+}-free solution (120

mM NaCl, 5.4 mM KCl, 1.2 mM $MgSO_4$, 1.2 mM KH_2PO_4, 6 mM HEPES, 10 mM glucose, and 10 mM taurine [pH adjusted to 7.4 using NaOH]) containing 1 mg/mL collagenase (Type I, Sigma) and 0.06 mg/mL proteinase (type XIV, Sigma). After the perfusion, the heart was disconnected from the cannula, cut into small pieces, and gently triturated with a plastic transfer pipette, and the homogenate was filtered through a nylon mesh. The dissociated cells were stored in normal Tyrode's solution at 20–22°C. Rod-shaped cells with clear striations and no granulation were used within 6–8 h for all the experiments.

2.3 H9c2 culture and plasmid transfection

The H9c2 rat myoblast cell line (BCRC60096) was purchased from the Bioresource Collection and Research Center of the Food Industry Research and Development Institute (Taiwan). The cells were cultured in Dulbecco's modified Eagle's medium (DMEM) supplemented with 10% of fetal bovine serum, 150 U/mL penicillin, and 150 mg/mL streptomycin. cDNAs of full-length wild type (WT) Sirt1 and mutant Sirt1 (H363Y) were cloned into the pSG5.HA vector[12]. The cells were incubated at 37°C in 5% CO_2/95% air. Confluent cells were detached with a 0.05% trypsin/0.02% EDTA solution and subcultured in 6-well culture plates to obtain the second passage. On the following day, the cells were plasmid-transfected by means of the Lipofectamine 3000 Reagent (Thermo Fisher Scientific Co., Carlsbad, CA, USA) according to the manufacturer's instructions. After 24 h transfection, the H9c2 cells were treated with 150 mM PA for 12 h.

2.4 Immunoblotting analysis

Ventricular tissues were homogenized in FastPrep-24 5G (MP Biomedicals) with RIPA buffer (100 mmol/L Tris-HCl pH 8.0, 0.1% of sodium dodecyl sulfate, 1% of Triton X-100, and 150 mmol/L NaCl) containing a protease inhibitor cocktail (Roche), followed by centrifugation at 15000 rpm for 15 min at 4°C. Protein content was determined in the supernatants, according to the DC Protein Assay instruction manual (Bio-Rad). H9c2 cells were lysed in RIPA buffer (100 mM Tris-HCl pH 8.0, 150 mM NaCl, 0.1% of SDS, and 1% of Triton X-100) and then centrifuged for 15 min at 15,000 rpm at 4°C. The protein extracts from heart tissue and from cultured H9c2 cells were separated by SDS polyacrylamide gel electrophoresis and then transferred to polyvinylidene difluoride membranes (Millipore), which were incubated with the following antibodies: anti-α-Tubulin (1:10000, Proteintech), anti-GAPDH (1:10000, Proteintech), anti-CHOP (1:800, Cell Signaling Technology), anti-ATF4 (1:800, Santa Cruz Biotechnology), anti-Sirt1 (1:800, Millipore), and anti-ac-H3K9 (1:1000, Merck). Immunoreactive proteins were detected via enhanced chemiluminescence (GE Healthcare) and quantified in the ImageJ software (NIH).

2.5 RT-PCR analysis

Total RNA was extracted from heart tissue and cultured H9c2 cells using the Total RNA reagent (Bioman, Taiwan, ROC). Next, 1 μg of total RNA was reverse-transcribed using the Moloney murine leukemia virus (MMLV) reverse transcriptase (Epicentre Biotechnologies, USA) as per the manufacturer's instructions. The resultant cDNA was quantified by quantitative RT-PCR in an Illumina ECO™ Real-Time PCR system. Cycle threshold (C_t) values for target mRNAs were normalized to the housekeeping gene *GAPDH*, and relative gene expression was calculated by the $2^{-\Delta\Delta Ct}$ method.

Primer sequences were as follows: *GAPDH* forward 5'-GGATACTGAGAGCAAGAGAGAGG-3' and reverse 5'-TCCTGTTGTTATGGGGTCTGG-3', *CHOP* forward 5'-ccagcagaggtcacaagcac-3' and reverse 5'-cgcactgaccactctgtttc-3', and *ATF4* forward 5'-CCTGACTCTGCTGCTTATATTACTCTAAC-3' and reverse 5'-ACTCCAGGTGGGTCATAAGGTTTG-3'.

2.6 Cellular NAD^+(H) levels, and cytoplasmic and nuclear extract preparation

The cytosolic NAD^+/NADH ratio was determined using the NAD^+/NADH Quantitation Colorimetric Kit (BioVision K337-100) as per the manufacturer's instructions. H9c2 cells were washed twice in ice-cold PBS and detached with PBS. After the removal of the supernatant, cytoplasmic and nuclear proteins were extracted from the cells by means of the Cytoplasmic and Nuclear Protein Extraction Kit (BIOTOOLS Co., Ltd. Taiwan), according to the manufacturer's instructions.

2.7 A chromatin immunoprecipitation (ChIP) assay

ChIP was performed with the SimpleChIP® Enzymatic Chromatin IP Kit (Cell Signaling Technology). Briefly, cells were incubated with 1% formaldehyde at room temperature for 10 min for cross-linking proteins to DNA. Chromatin was sonicated, and 10 mg of it was subjected to immunoprecipitation with antibodies [anti-ATF4 (Santa Cruz Biotechnology), anti-ac-H3K9 (Merck), or negative control (Normal Mouse IgG; Cell Signaling Technology)] at 4°C overnight with rotation. The following day, chromatin/antibody complexes were pulled down from the solution by incubation with salmon sperm DNA–saturated 50% protein A/G–Sepharose beads at 4°C for 2 h. The cross-linking was reversed by heating at 65°C for 30 min, followed by treatment with 100 g/L proteinase K at 65°C for 2 h. DNA purification was performed using the kit mentioned above, and the purified DNA was analyzed by PCR. The primers for *CHOP* were forward 5'-AAGTTCAGGAAGGACAGCCG-3' and reverse 5'-CGTTATCTCGGACCCGGAAG-3'.

2.8 Acquisition systems and statistical analysis

Continuous variables were expressed as the mean ± standard error of the mean. Student's *t*-test or Pearson's Chi-square test was performed to evaluate the differences. GraphPad Prism 5 (Systat Software Inc., USA) was used for statistical comparisons. In figures, "n" stands for the total number of cells per heart (n = cells/hearts), and "N" is the number of mice. Statistical significance is indicated by *, **, and *** for $P < 0.05$, $P < 0.01$, and $P < 0.001$, respectively.

3 Results

3.1 The induction of CHOP and ATF4 expression in cardiomyocytes of mice and H9c2 cells by HFD and PA, respectively

The HFD is one of the inducers of ER stress[13,14]. To address the role of Sirt1 in HFD-induced ER stress in cardiomyocytes, we fed 8-week-old $Sirt1^{f/f}$ and $Sirt1^{-/-}$ mice with HFD for 8 weeks. CHOP and ATF4 protein levels and mRNA expression were higher in the control mice fed with the HFD compared to those fed the SD (Fig. 1A, B & C). $Sirt1^{-/-}$ mice showed increased protein levels and mRNA expression of CHOP and ATF4 as compared to the control mice fed either the SD or HFD (Fig. 1B & C). We exposed H9c2 cells to PA and investigated the expression of CHOP and ATF4. The protein levels and mRNA expression of both ATF4 and CHOP in H9c2 cells were significantly increased by the PA treatment in a dose-dependent manner (Fig. 2A, B & C) and in a time-dependent manner (Fig. 2D, E & F).

3.2 Palmitate decreases Sirt1's deacetylating activity mediated by the downregulation of cytosolic NAD^+ in H9c2 cells

Sirt1 is known to deacetylate acetyl-lysine in histones, e.g., H3K9Ac, to modulate gene transcription[15]. To investigate the function of Sirt1 under PA-induced ER stress in H9c2 cells, we quantified Sirt1 protein expression and acetyl-lysine9 in histone H3 (H3K9Ac), a primary target of Sirt1. While the protein level of Sirt1 remained unchanged, the level of H3K9Ac significantly increased in a dose-dependent and time-dependent manner in H9c2 cells after the treatment with PA (see Fig. 3A & B for the dose-course experiment and Fig. 3C & D for the time-course experiment). The increased H3K9Ac amount implied decreased enzymatic activity of Sirt1 not mediated by the downregulation of the Sirt1 protein amount. We next examined whether the cellular NAD^+/NADH ratio was affected, which may be responsible for the reduced deacetylating activity of Sirt1, under PA-induced ER stress. Our data showed that NAD^+/NADH ratios significantly decreased in H9c2 cells treated with PA in a dose-dependent manner (Fig. 3E).

3.3 Sirt1 reduces mRNA and protein expression of ATF4 and CHOP in H9c2 cells

It is important to verify the decreased ratio of NAD^+ to NADH for assessing Sirt1's deacetylating enzymatic activity. One dominant negative Sirt1 mutant (H363Y) has been found to lose the deacetylating activity[16]. Hence, we suppressed the enzymatic activity of Sirt1 via this dominant negative H363Y mutation in H9c2 cells to determine whether the abrogation of Sirt1 enzymatic activity affects the expression of CHOP and ATF4. Sirt1 H363Y induced mRNA and protein expression of CHOP and ATF4 in H9c2 cells (Fig. 4A & B). After PA treatment, the protein expression of CHOP and ATF4 increased in Sirt1 H363Y–transfected H9c2 cells (Fig. 4C & D). On the contrary, the H3K9Ac upregulation by Sirt1 H363Y was attenuated by the PA treatment.

3.4 SRT1720 enhances nuclear translocation of ATF4 and reduces histone H3 K9 acetylation in the CHOP promoter

Our above-mentioned data indicated that PA reduces the cytosolic NAD^+ amount thereby suppressing the enzymatic activity of Sirt1 in H9c2 cells. Accordingly, we applied a Sirt1 activator, SRT1720, to address the role of the deacetylating activity of Sirt1 in the regulation of ATF4 and CHOP expression in H9c2 cells. SRT1720 did not suppress mRNA expression of CHOP and ATF4 in PA-treated H9c2 cells (Fig. 5A). SRT1720 reduced the levels of H3K9Ac in PA-treated H9c2 cells, suggesting that it is an activator of Sirt1's deacetylating activity (Fig. 5B). Under ER stress, ATF4 may migrate to the nucleus, bind to target genes, and regulate their transcription[17]. Next, we tested whether SRT1720 affects the cytosolic and nuclear fractions of Sirt1 and ATF4 in H9c2 cells treated or not treated with PA. Nuclear translocation of ATF4 in H9c2 cells was increased by the PA treatment and further strengthened when combined with SRT1720 treatment (Fig. 5C & D). Neither PA nor SRT1720 influenced the cytosolic and nuclear fractions of Sirt1 (Fig. 5C & D). The ChIP results showed that in H9c2 cells, PA induced the recruitment of ATF4 to the *CHOP* promoter (1.84% vs. 3.49%), but this effect was not further enhanced by the combination with SRT1720 treatment (3.49% vs. 3.54%) (Fig. 5E & F). SRT1720 significantly lowered the amount of H3K9Ac in the CHOP promoter in PA-treated H9c2 cells (4.22% vs. 2.35%) (Fig. 5E & F).

4 Discussion

Lipotoxicity is an important contributor to cardiac dysfunction in obesity-associated heart disease[18,19]. Excessive uptake of fatty acids can result in either enhanced oxidation or abnormal accumulation of toxic lipid species such as ceramides and diacylglycerides, causing lipotoxicity in the heart and other solid organs, and the one of crucial underlying mechanism is ER stress and impaired UPR signaling[20]. Some evidence indicates that the activation of Sirt1/AMPK signaling may prevent cells from fatty-acid–induced oxidative stress and inflammation[21], but the participation of Sirt1 in lipotoxicity-induced ER stress remains unclear. In the present study, we utilized mice fed a palmitate-enriched HFD and palmitate-treated H9c2 cells as *in vivo* and *in vitro* models of lipotoxicity and examined the cellular consequences, including ER stress and Sirt1 activity, as well as the crosstalk between these cellular phenomena.

There are studies showing that the lipotoxicity associated with ER stress increases *ATF4* and *CHOP* mRNA expression, but the underlying mechanism still needs to be clarified[20,22,23]. Our data revealed that palmitate induces the expression of ER stress markers CHOP and ATF4 *in vivo* and *in vitro*, in line with other reports[20,22,23]. One study suggests that palmitate-induced cardiomyocyte dysfunction is mediated by ER stress and thereby promotes cell death[3]. Sirt1 may confer cardioprotection against ER stress. Alexandre et al. have reported that cardiac Sirt1 deficiency increases the contractile dysfunction caused by ER stress in a Sirt1 knockout mouse model, and the mechanism may involve eIF2α deacetylation[24]. According to our results, $Sirt1^{-/-}$ cardiomyocytes show higher expression of CHOP and ATF4 as compared to cardiomyocytes from the control mice fed either the SD or HFD, also suggesting a protective role of Sirt1 against HFD-induced ER stress in cardiomyocytes.

As an NAD^+-dependent reaction, the protein deacetylation catalyzed by Sirt1 is accompanied by the hydrolysis of NAD^+. Therefore, we propose that the decreased Sirt1 activity is associated with reduced

NAD^+ concentration in palmitate-treated H9c2 cells, in line with other reports[25,26]. Some research has revealed that changes in cytosolic NAD^+ levels alter Sirt1 activity[27–29]. Additionally, one report has shown that reduced cellular NAD^+ concentration, resulting from the conversion of NAD^+ to NADH by the glucose metabolic pathway, leads to lower Sirt1 activity[30]. As a consequence of its dependence on NAD^+ and therefore on the cellular NAD^+/NADH ratio, Sirt1 has emerged as a key metabolic sensor with respect to various tissues[31]. There is evidence[32,33] that in a high-energy state, such as that associated with an HFD and obesity, Sirt1 activity may decline with a decreased level of NAD^+. Therefore, we propose that palmitate-induced ER stress diminishes the cytosolic level of NAD^+, which in turn reduces Sirt1 enzymatic activity.

Our results indicate that the dominant negative Sirt1 H363Y mutant increases the expression of ATF4 and CHOP, also implying a protective role of Sirt1 (via its enzymatic activity) against ER stress[24]. Nevertheless, PA did not raise either ATF4 or CHOP expression in the H9c2 cells transfected with the plasmid encoding the Sirt1 H363Y mutant, and the same was true for H3K9Ac. We believe that the plasmid transfection of H9c2 cells attenuates the influence of PA or PA weakens the effects of the plasmid transfection. In addition, our data indicate that autophagy-related proteins beclin 1 and p63 are upregulated in the H9c2 cells treated with PA (Supplemental Data 1). PA-induced autophagy has been shown to abrogate the partial apoptosis caused by PA[34]. Therefore, ATF4 or CHOP expression in the H9c2 cells transfected with the Sirt1 H363Y mutant may be abrogated by the autophagy induced by PA. The increase in the H3K9Ac level in PA-treated H9c2 cells was attenuated by SRT1720 treatment, implying increased deacetylation function of Sirt1, although NAD^+ concentration was not restored under these conditions. On the other hand, the PA-induced expression of ATF4 was not weakened by SRT1720 treatment. Furthermore, our findings show that the translocation of ATF4 to the nucleus increases upon SRT1720 treatment; as a consequence, the increased nuclear recruitment may enhance the gene-regulatory function of ATF4. With PA treatment, there was more binding between ATF4 and the *CHOP* promoter. By contrast, with PA plus SRT1720 treatment, the extent of binding between ATF4 and the *CHOP* promoter did not increase further, although SRT1720 made more ATF4 available in the nucleus. SRT1720 strengthened the activity of Sirt1 but had only a limited impact on the CHOP and ATF4 expression induced by PA treatment, suggesting involvement of more than a deacetylating activity. The protein–protein interaction and nuclear localization are being researched in more detail to decipher the current complicated findings.

In conclusion, PA-induced ER stress may be mediated by the upregulation of ATF4 and CHOP mRNAs and proteins. PA reduces the amount of cytosolic NAD^+, which in turn suppresses Sirt1 activity. Nevertheless, the Sirt1 activator SRT1720 does not attenuate the expression of CHOP and ATF4 induced by PA but enhances nuclear translocation of ATF4.

Declarations

Acknowledgements

We thank Elsevier Author Services (https://webshop.elsevier.com/language-editing-services/) for the English-editing service.

Author contributions

H.-Y. Yang, J.-Y. Chen, and P.-L. Yu conducted the experiments; H.-Y. Yang, J.-Y. Chen, Y.-N. Huo, and S.-C. Hsu analyzed the data. H.-Y. Yang, Y.-N. Huo, S.-C. Hsu, and S.-M. Huang interpreted the results of the experiments; J.-Y. Chen and P.-L. Yu prepared the figures; H.-Y. Yang drafted the manuscript; H.-Y. Yang and S.-M. Huang edited and revised the manuscript; C.-S. Tsai and C.-Y. Lin conceived and designed the study. All the authors approved the final version of the manuscript.

Funding information

This work was supported by Ministry of Science and Technology of Taiwan (MOST-107-2314-B-016-063-MY3 and MOST108–2314-B-016-050); Veterans General Hospital at Taipei Taichung and Kaohsiung, Tri-Service General Hospital, and Academia Sinica Joint Research Program (VTA109-V1-3-2); Tri-Service General Hospital, Taiwan (TSGH-C01-110018 and TSGH-E-109209).

Data availability statement

The data of the present study are available from the corresponding authors upon reasonable request.

Conflict of interest

The authors declare no conflict of interest.

References

1. Nakamura, M. & Sadoshima, J. Cardiomyopathy in obesity, insulin resistance and diabetes. *The Journal of physiology* **598**, 2977-2993, doi:10.1113/jp276747 (2020).
2. Drosatos, K. & Schulze, P. C. Cardiac lipotoxicity: molecular pathways and therapeutic implications. *Current heart failure reports* **10**, 109-121, doi:10.1007/s11897-013-0133-0 (2013).
3. Yang, L. *et al.* Oxidative and endoplasmic reticulum stresses are involved in palmitic acid-induced H9c2 cell apoptosis. *Bioscience reports* **39**, doi:10.1042/bsr20190225 (2019).
4. Xu, C., Bailly-Maitre, B. & Reed, J. C. Endoplasmic reticulum stress: cell life and death decisions. *The Journal of clinical investigation* **115**, 2656-2664, doi:10.1172/jci26373 (2005).
5. Matsushima, S. & Sadoshima, J. The role of sirtuins in cardiac disease. *American journal of physiology. Heart and circulatory physiology* **309**, H1375-1389, doi:10.1152/ajpheart.00053.2015 (2015).
6. Sanz, M. N. *et al.* Inducible Cardiac-Specific Deletion of Sirt1 in Male Mice Reveals Progressive Cardiac Dysfunction and Sensitization of the Heart to Pressure Overload. *International journal of molecular sciences* **20**, doi:10.3390/ijms20205005 (2019).

7. Gorski, P. A. *et al.* Role of SIRT1 in Modulating Acetylation of the Sarco-Endoplasmic Reticulum Ca(2+)-ATPase in Heart Failure. *Circulation research* **124**, e63-e80, doi:10.1161/circresaha.118.313865 (2019).
8. Bugyei-Twum, A. *et al.* Sirtuin 1 activation attenuates cardiac fibrosis in a rodent pressure overload model by modifying Smad2/3 transactivation. *Cardiovascular research* **114**, 1629-1641, doi:10.1093/cvr/cvy131 (2018).
9. Prola, A. *et al.* SIRT1 protects the heart from ER stress-induced cell death through eIF2α deacetylation. *Cell Death & Differentiation* **24**, 343-356, doi:10.1038/cdd.2016.138 (2017).
10. Hsu, Y. J. *et al.* Sirtuin 1 protects the aging heart from contractile dysfunction mediated through the inhibition of endoplasmic reticulum stress-mediated apoptosis in cardiac-specific Sirtuin 1 knockout mouse model. *International journal of cardiology* **228**, 543-552, doi:10.1016/j.ijcard.2016.11.247 (2017).
11. Weng, C. H. *et al.* Pleiotropic Effects of Myocardial MMP-9 Inhibition to Prevent Ventricular Arrhythmia. *Scientific reports* **6**, 38894, doi:10.1038/srep38894 (2016).
12. Amat, R. *et al.* SIRT1 controls the transcription of the peroxisome proliferator-activated receptor-gamma Co-activator-1alpha (PGC-1alpha) gene in skeletal muscle through the PGC-1alpha autoregulatory loop and interaction with MyoD. *The Journal of biological chemistry* **284**, 21872-21880, doi:10.1074/jbc.M109.022749 (2009).
13. Hsu, H. C., Chen, C. Y., Lee, B. C. & Chen, M. F. High-fat diet induces cardiomyocyte apoptosis via the inhibition of autophagy. *European journal of nutrition* **55**, 2245-2254, doi:10.1007/s00394-015-1034-7 (2016).
14. Tan, L., Harper, L., McNulty, M. A., Carlson, C. S. & Yammani, R. R. High-fat diet induces endoplasmic reticulum stress to promote chondrocyte apoptosis in mouse knee joints. *FASEB journal : official publication of the Federation of American Societies for Experimental Biology* **34**, 5818-5826, doi:10.1096/fj.201902746R (2020).
15. Yang, G. *et al.* The histone H3K9 methyltransferase SUV39H links SIRT1 repression to myocardial infarction. *Nature communications* **8**, 14941, doi:10.1038/ncomms14941 (2017).
16. Suter, M. A. *et al.* A maternal high-fat diet modulates fetal SIRT1 histone and protein deacetylase activity in nonhuman primates. *FASEB journal : official publication of the Federation of American Societies for Experimental Biology* **26**, 5106-5114, doi:10.1096/fj.12-212878 (2012).
17. Han, J. *et al.* ER-stress-induced transcriptional regulation increases protein synthesis leading to cell death. *Nature cell biology* **15**, 481-490, doi:10.1038/ncb2738 (2013).
18. Leroy, C., Tricot, S., Lacour, B. & Grynberg, A. Protective effect of eicosapentaenoic acid on palmitate-induced apoptosis in neonatal cardiomyocytes. *Biochimica et biophysica acta* **1781**, 685-693, doi:10.1016/j.bbalip.2008.07.009 (2008).
19. Wende, A. R. & Abel, E. D. Lipotoxicity in the heart. *Biochimica et biophysica acta* **1801**, 311-319, doi:10.1016/j.bbalip.2009.09.023 (2010).

20. Han, J. & Kaufman, R. J. The role of ER stress in lipid metabolism and lipotoxicity. *Journal of lipid research* **57**, 1329-1338, doi:10.1194/jlr.R067595 (2016).
21. Xu, H. *et al.* Hepatic Proteomic Changes and Sirt1/AMPK Signaling Activation by Oxymatrine Treatment in Rats With Non-alcoholic Steatosis. *Frontiers in pharmacology* **11**, 216, doi:10.3389/fphar.2020.00216 (2020).
22. Fusakio, M. E. *et al.* Transcription factor ATF4 directs basal and stress-induced gene expression in the unfolded protein response and cholesterol metabolism in the liver. *Molecular biology of the cell* **27**, 1536-1551, doi:10.1091/mbc.E16-01-0039 (2016).
23. Wortel, I. M. N., van der Meer, L. T., Kilberg, M. S. & van Leeuwen, F. N. Surviving Stress: Modulation of ATF4-Mediated Stress Responses in Normal and Malignant Cells. *Trends in endocrinology and metabolism: TEM* **28**, 794-806, doi:10.1016/j.tem.2017.07.003 (2017).
24. Prola, A. *et al.* SIRT1 protects the heart from ER stress-induced cell death through eIF2α deacetylation. *Cell death and differentiation* **24**, 343-356, doi:10.1038/cdd.2016.138 (2017).
25. Flores-León, M., Pérez-Domínguez, M., González-Barrios, R. & Arias, C. Palmitic Acid-Induced NAD(+) Depletion is Associated with the Reduced Function of SIRT1 and Increased Expression of BACE1 in Hippocampal Neurons. *Neurochemical research* **44**, 1745-1754, doi:10.1007/s11064-019-02810-8 (2019).
26. Shen, C. *et al.* Nicotinamide protects hepatocytes against palmitate-induced lipotoxicity via SIRT1-dependent autophagy induction. *Nutrition research (New York, N.Y.)* **40**, 40-47, doi:10.1016/j.nutres.2017.03.005 (2017).
27. Li, J. *et al.* Nicotinamide ameliorates palmitate-induced ER stress in hepatocytes via cAMP/PKA/CREB pathway-dependent Sirt1 upregulation. *Biochimica et biophysica acta* **1853**, 2929-2936, doi:10.1016/j.bbamcr.2015.09.003 (2015).
28. Cantó, C. *et al.* AMPK regulates energy expenditure by modulating NAD+ metabolism and SIRT1 activity. *Nature* **458**, 1056-1060, doi:10.1038/nature07813 (2009).
29. Yoshino, J., Mills, K. F., Yoon, M. J. & Imai, S. Nicotinamide mononucleotide, a key NAD(+) intermediate, treats the pathophysiology of diet- and age-induced diabetes in mice. *Cell metabolism* **14**, 528-536, doi:10.1016/j.cmet.2011.08.014 (2011).
30. Cantó, C., Menzies, K. J. & Auwerx, J. NAD(+) Metabolism and the Control of Energy Homeostasis: A Balancing Act between Mitochondria and the Nucleus. *Cell metabolism* **22**, 31-53, doi:10.1016/j.cmet.2015.05.023 (2015).
31. Anderson, K. A., Madsen, A. S., Olsen, C. A. & Hirschey, M. D. Metabolic control by sirtuins and other enzymes that sense NAD(+), NADH, or their ratio. *Biochimica et biophysica acta. Bioenergetics* **1858**, 991-998, doi:10.1016/j.bbabio.2017.09.005 (2017).
32. Li, X. SIRT1 and energy metabolism. *Acta biochimica et biophysica Sinica* **45**, 51-60, doi:10.1093/abbs/gms108 (2013).
33. Schug, T. T. & Li, X. Sirtuin 1 in lipid metabolism and obesity. *Annals of medicine* **43**, 198-211, doi:10.3109/07853890.2010.547211 (2011).

34. Jiang, X. S. *et al.* Autophagy Protects against Palmitic Acid-Induced Apoptosis in Podocytes in vitro. *Scientific reports* **7**, 42764, doi:10.1038/srep42764 (2017).

Figures

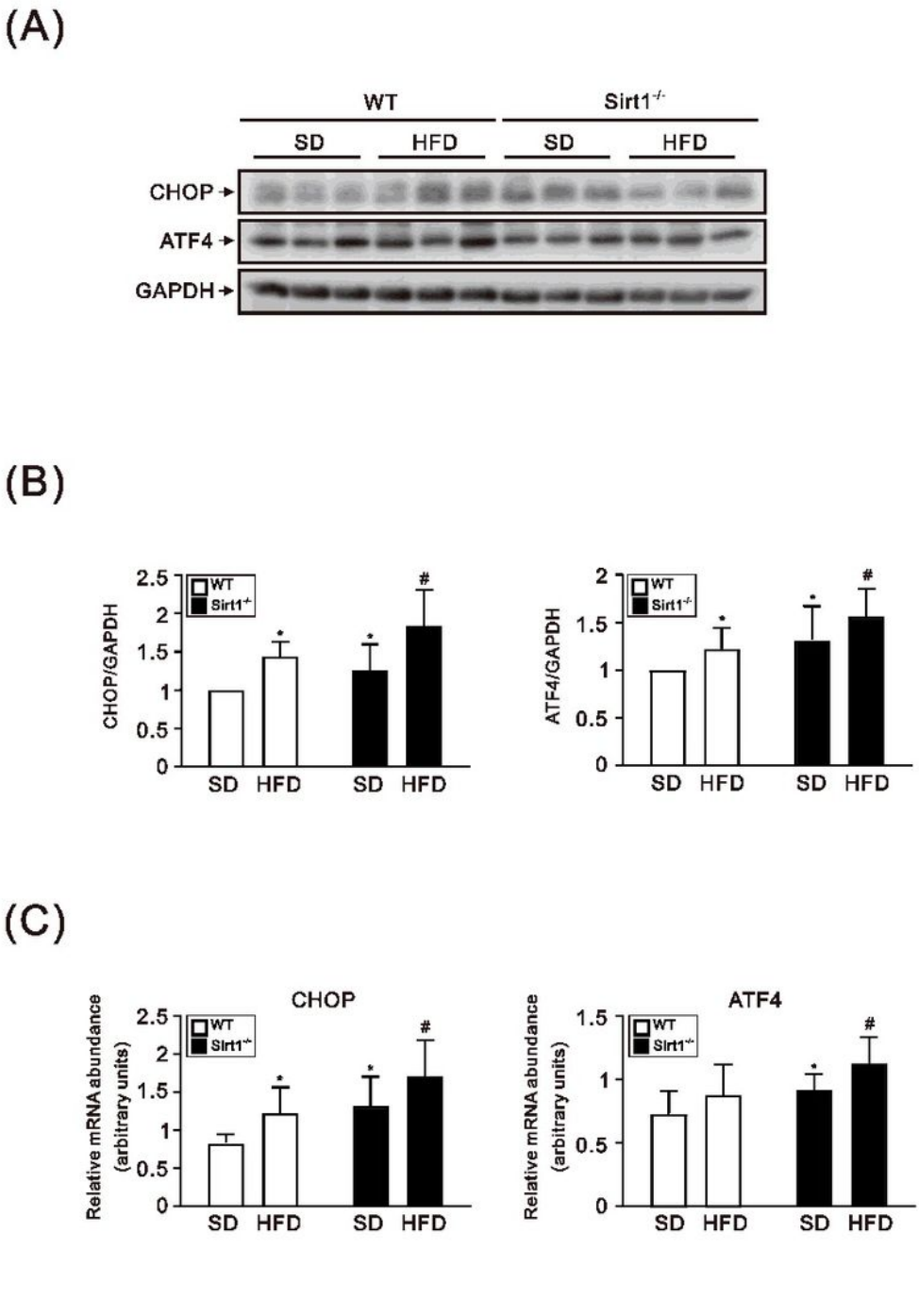

Figure 1

Protein levels and mRNA expression of CHOP and ATF4 in ventricular tissues from control and Sirt1-/- mice fed either the SD or HFD. (A) A representative immunoblot of CHOP and ATF4 in control and Sirt1-/- mice fed with either the SD or HFD. (B) The HFD increased protein levels of CHOP and ATF4 in WT mice as compared to those fed with the SD. The protein levels of CHOP and ATF4 were higher in Sirt1-/- mice compared to the control mice fed either the SD or HFD (N = 6; *compared to WT mice on the SD, #compared to WT mice on the HFD ; *P < 0.05; #P < 0.05). (C) Relative mRNA expression of CHOP and ATF4 was higher in Sirt1-/- mice compared to the control mice fed with either the SD or HFD (N = 6; *compared to WT mice on the SD, #compared to WT mice on the HFD; *P < 0.05; #P < 0.05).

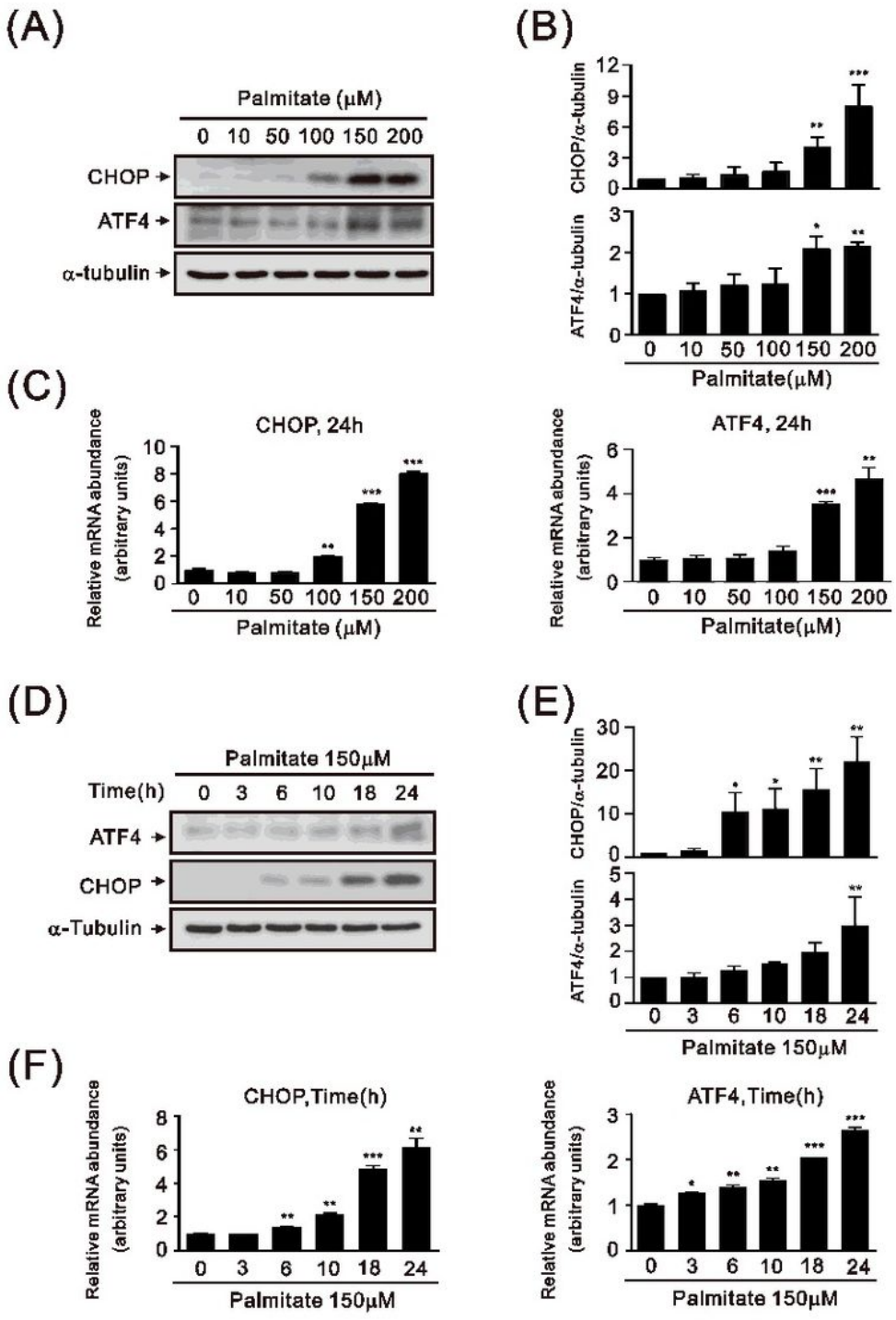

Figure 2

Protein levels and mRNA expression of CHOP and ATF4 in the H9c2 cells treated with PA. (A) A representative immunoblot and (B) mean data for CHOP and ATF4 in the H9c2 cells treated with PA (0–200 μM) at 24 h (n = 3; asterisk(s): compared to the 0 μM PA control group; *P < 0.05, **P < 0.01, ***P < 0.001). (C) Relative levels of CHOP and ATF4 mRNAs in H9c2 cells after PA (0–200 μM) treatment at 24 h (n = 3; asterisk(s): compared to the 0 μM PA control group; **P < 0.01, ***P < 0.001). (D) A representative

immunoblot and (E) mean data for CHOP and ATF4 in H9c2 cells treated with PA (150 μM, 0–24 h) (n = 3; asterisk(s): compared to the 0 μM PA control group; *P < 0.05, **P < 0.01). (F) Relative expression levels of CHOP and ATF4 mRNA in H9c2 cells after PA (150 μM, 0–24 h) treatment (n = 2; asterisk(s): compared to the 0 μM PA control group; *P < 0.05, **P < 0.01, ***P < 0.001).

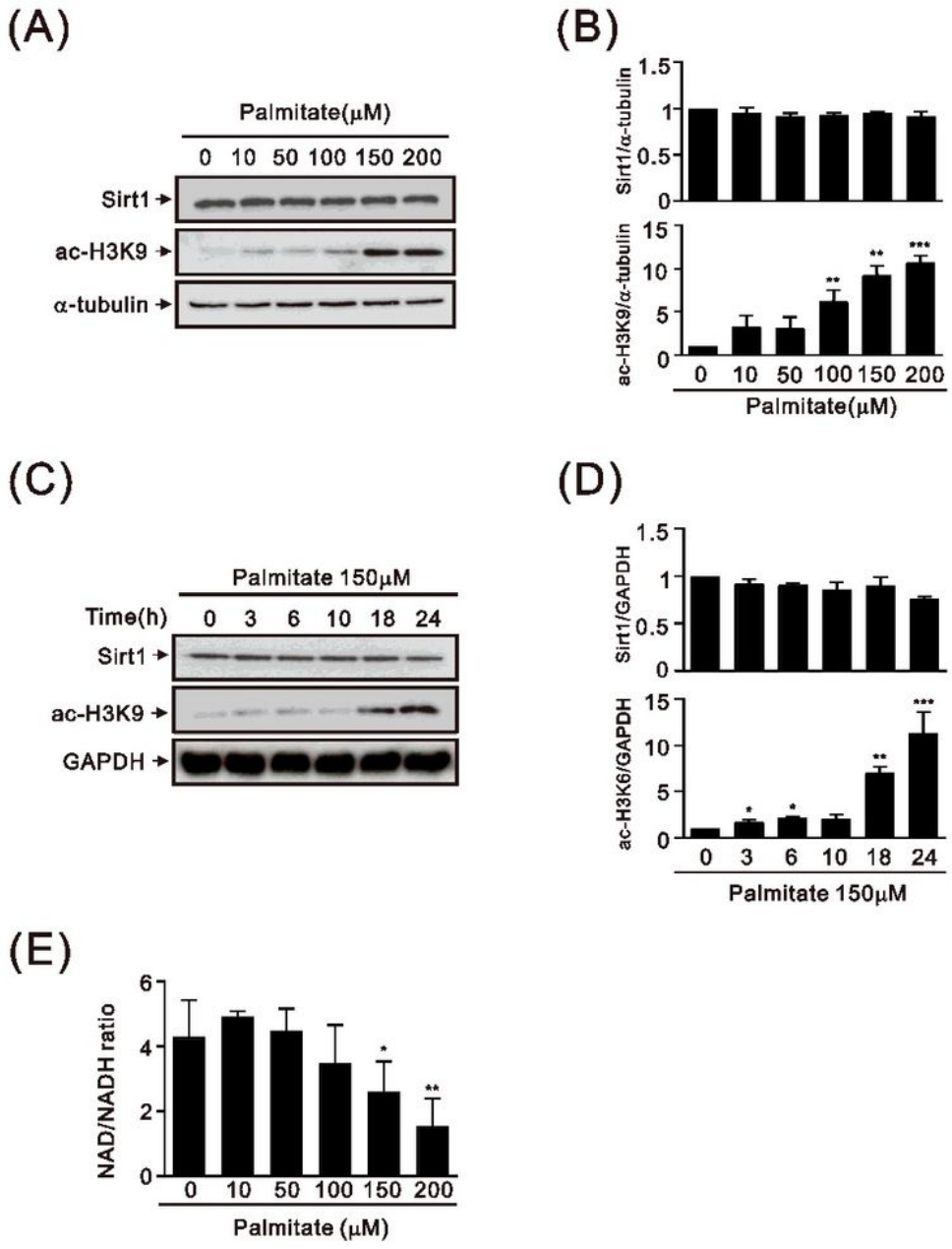

Figure 3

Protein levels of Sirt1, the H3K9Ac amount, and the cytosolic NAD+/NADH ratio in H9c2 cells treated with PA. (A) A representative immunoblot and (B) mean data for Sirt1 and H3K9Ac in H9c2 cells treated with PA (0–200 μM) at 24 h (n = 3; asterisk: compared to the 0 μM PA control group; **P < 0.01, ***P < 0.001). (C) A representative immunoblot and (D) mean data for Sirt1 and H3K9Ac in H9c2 cells treated with PA (150 μM, 0–24 h) (n = 3; asterisk(s): compared to the 0 μM PA control group; **P < 0.01, ***P < 0.001). (E) The cytosolic NAD+/NADH ratio in the H9c2 cells treated with PA decreased in a PA dose–dependent manner (n = 3; *P < 0.05, **P < 0.01).

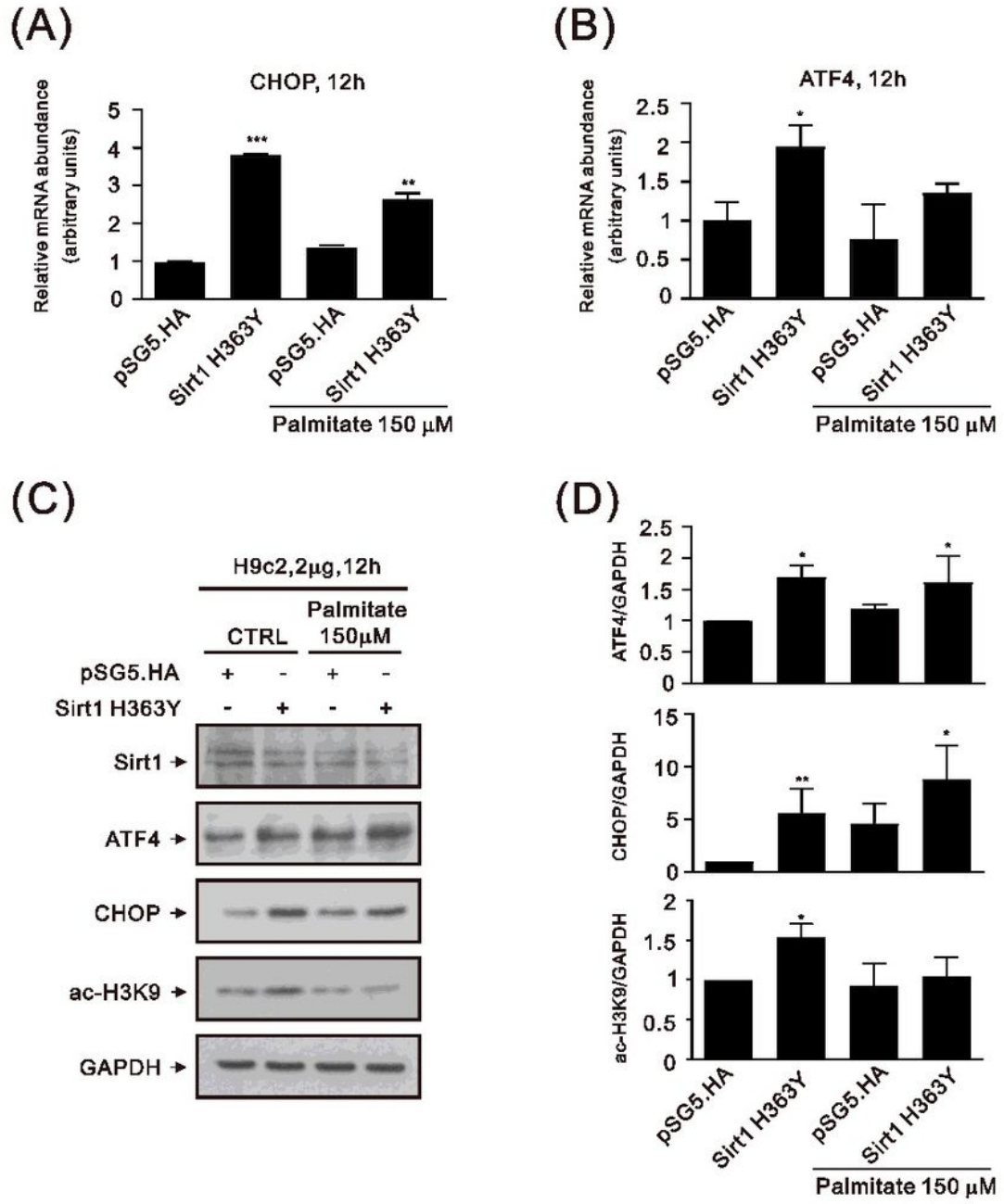

Figure 4

Effects of transfection with the plasmid encoding the Sirt1 H363Y mutant in H9c2 cells. (A) & (B) Relative mRNA expression of CHOP and ATF4 in pSG5.HA- or H363Y mutant Sirt1 plasmid–transfected H9c2 cells treated or not treated with PA (n = 2; asterisk(s): compared to the pSG5.HA group; *P < 0.05 and ***P < 0.001). (C) & (D) The protein expression of CHOP and ATF4 in pSG5.HA- or H363Y mutant Sirt1 plasmid–transfected H9c2 cells treated or not treated with PA (n = 3; asterisk(s): compared to the pSG5.HA group; *P < 0.05 and **P < 0.01)

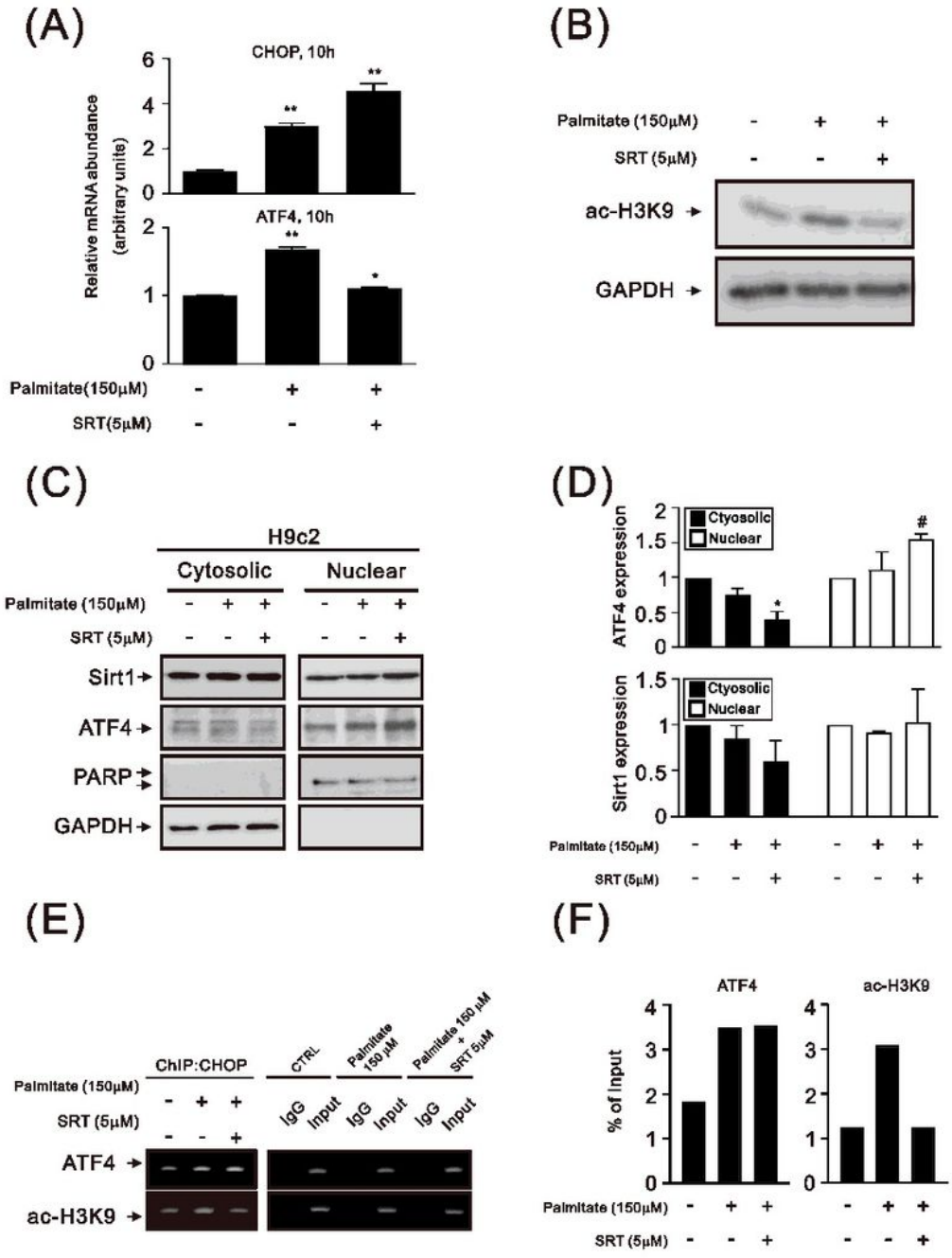

Figure 5

Effects of SRT1720 on CHOP and ATF4 in the H9c2 cells treated with PA. (A) The relative mRNA expression of CHOP in PA-treated H9c2 cells with or without SRT1720 (n = 2; *P < 0.05, **P < 0.01). (B) A representative immunoblot of ATF4 and H3K9Ac in PA-treated H9c2 cells with or without SRT1720 (n = 3, *P < 0.05; SRT: SRT1720). (C) & (D) The expression of ATF4 and Sirt1 in cytosolic and nuclear fractions (n = 3; *compared to the cytosol control; #compared to the nuclear control; *P < 0.05, #P < 0.05). (E) & (F) ChIP for assessing the interaction between ATF4 and the CHOP promotor and between H3K9ac and the CHOP promotor in PA-treated H9c2 cells with or without SRT1720 (ATF4/CHOP promotor: 1.84%, 3.49%, and 3.54%, respectively; H3K9ac/CHOP promotor: 2.33%, 4.22%, and 2.35%, respectively; n = 1)

Supplementary Files

This is a list of supplementary files associated with this preprint. Click to download.

- Sup.tif
- Supplementaldata1.docx